The Intramembrane Protease SPPL2A Is Critical for Tooth Enamel Formation

Antonius LJJ Bronckers,[1,2] Nur Gueneli,[3] Renate Lüllmann-Rauch,[4] Janna Schneppenheim,[3] Andreea P Moraru,[1,2] Nina Himmerkus,[5] Theodore J Bervoets,[1,2] Regina Fluhrer,[6,7] Vincent Everts,[1,2] Paul Saftig,[3] and Bernd Schröder[3]

[1]Department of Oral Cell Biology ACTA, University of Amsterdam, Amsterdam, The Netherlands
[2]VU-University of Amsterdam, Research Institute MOVE, Amsterdam, The Netherlands
[3]Biochemical Institute, Christian-Albrechts-University of Kiel, Kiel, Germany
[4]Institute of Anatomy, Christian-Albrechts-University of Kiel, Kiel, Germany
[5]Physiological Institute, Christian-Albrechts-University of Kiel, Kiel, Germany
[6]Adolf-Butenandt-Institute for Biochemistry, Ludwig Maximilians University Munich, Munich, Germany
[7]German Center for Neurodegenerative Diseases (DZNE), Munich, Germany

ABSTRACT

Intramembrane proteases are critically involved in signal transduction and membrane protein turnover. Signal-peptide-peptidase-like 2a (SPPL2A), a presenilin-homologue residing in lysosomes/late endosomes, cleaves type II-oriented transmembrane proteins. We recently identified SPPL2A as the enzyme controlling turnover and functions of the invariant chain (CD74) of the major histocompatibility complex II (MHCII) and demonstrated critical importance of this process for B cell development. Surprisingly, we found that SPPL2A is critical for formation of dental enamel. In *Sppl2a* knockout mice, enamel of the erupted incisors was chalky white and rapidly eroded after eruption. SPPL2A was found to be expressed in enamel epithelium during secretory and maturation stage amelogenesis. Mineral content of enamel in $Sppl2a^{-/-}$ incisors was inhomogeneous and reduced by ~20% compared to wild-type mice with the most pronounced reduction at the mesial side. Frequently, disruption of the enamel layer and localized detachment of the most superficial enamel layer was observed in the knockout incisors leading to an uneven enamel surface. In *Sppl2a* null mice, morphology and function of secretory stage ameloblasts were not noticeably different from that of wild-type mice. However, maturation stage ameloblasts showed reduced height and a characteristic undulation of the ameloblast layer with localized adherence of the cells to the outer enamel. This was reflected in a delayed and incomplete resorption of the proteinaceous enamel matrix. Thus, we conclude that intramembrane proteolysis by SPPL2A is essential for maintaining cellular homeostasis of ameloblasts. Because modulation of SPPL2A activity appears to be an attractive therapeutic target to deplete B cells and treat autoimmunity, interference with tooth enamel formation should be investigated as a possible adverse effect of pharmacological SPPL2A inhibitors in humans. © 2013 American Society for Bone and Mineral Research.

KEY WORDS: INTRAMEMBRANE PROTEOLYSIS; SIGNAL-PEPTIDE-PEPTIDASE-LIKE 2A; MATURATION AMELOBLASTS; ENAMEL MATRIX RESORPTION; ENAMEL MINERALIZATION

Introduction

Regulated intramembrane proteolysis (RIP) refers to a sequential processing of transmembrane substrates. This involves the proteolytic release of an ectodomain (shedding) followed by further cleavage of the remaining membrane-bound fragment by an intramembrane protease (I-CLIP) that liberates an intracellular fragment.[1] In several cases, RIP cleavage products have been shown to transduce signals indicating the critical importance of this process for cell differentiation and development[2] as exemplified by the Notch signaling pathway.[3]

The signal-peptide-peptidase/signal-peptide-peptidase-like (SPP/SPPL) proteases belong to the aspartyl I-CLIPs[4] and were demonstrated to show specificity for transmembrane

Address correspondence to: Antonius LJJ Bronckers, Oral Cell Biology, ACTA Vrije Universiteit Gustav Mahlerlaan, 3004 1081 LA Amsterdam, Amsterdam, The Netherlands. E-mail: a.bronckers@acta.nl or Dr Bernd Schröder, Otto-Hahn-Platz 9, Christian-Albrechts-University Kiel, D-24118 Kiel Germany. E-mail: baschroeder@biochem.uni-kiel.de

Additional Supporting Information may be found in the online version of this article.

proteins in type 2 orientation.[5] With a predominant localization in membranes of lysosomes and late endosomes,[6,7] signal-peptide-peptidase-like 2a (SPPL2A) appears to be distinct from the other SPPL family members, suggesting unique functions of this protease. We recently identified SPPL2A as the long-sought protease mediating turnover and controlling functions of the invariant chain (CD74) of the major histocompatibility complex class II (MHCII).[8] We could show that this process is essential for B cell development. *Sppl2a* null mice exhibit a characteristic developmental block during the splenic phase of B cell maturation leading to a significant reduction of mature and functionally competent B cells and impairment of humoral immune responses in these mice. Based on a significant alleviation of this phenotype in *Sppl2a-Cd74* double-knockout mice, we unambiguously demonstrated that the accumulation of a CD74 N-terminal fragment (NTF) is responsible for the loss of B cells in $Sppl2a^{-/-}$ mice relating to its ability to disturb endocytic membrane traffic and central signaling pathways.

Because $Sppl2a^{-/-}$ mice do not appear to be overtly compromised, modulation of SPPL2A activity seems to be a promising pharmacological target to specifically deplete B cells and treat autoimmunity. In order to assess putative unrecognized adverse effects of such a therapeutic strategy, we are systematically analyzing additional consequences of SPPL2A deficiency. Surprisingly, we observed that SPPL2A is critical for formation of dental enamel. In developing teeth, enamel is generated by epithelial cells called ameloblasts in a sequential process.[9] In a first step, the secretory phase, these cells deposit a proteinaceous matrix that provides a scaffold for crystal growth. In the subsequent maturation stage, the ameloblasts develop significant resorptive and ion transporting capacities in order to mediate the complete reabsorption and removal of the matrix from the enamel space, which is a prerequisite for the successful completion of enamel mineralization.[9]

Here we report that enamel of incisors in $Sppl2a^{-/-}$ mice is decolorized and of reduced mechanical strength as illustrated by its rapid erosion after tooth eruption. Consistently, we demonstrate that SPPL2A is expressed in dental epithelium of wild-type mice during secretory and maturation stage amelogenesis and that enamel in *Sppl2a* null mice exhibits significantly reduced mineralization. This is due to a delayed and apparently incomplete resorption of enamel matrix during maturation stage, which is accompanied by characteristic structural changes of maturation stage ameloblasts in $Sppl2a^{-/-}$ mice. According to our knowledge, this is the first report that the action of an intramembrane protease is essential for ameloblast function and enamel formation.

Subjects and Methods

Animals

The generation of *Sppl2a* null mice (C57BL/6) has been reported.[8] In brief, a neomycin resistance cassette was inserted in exon 2 of the gene. Absence of *Sppl2a* wild-type transcript as well as SPPL2A protein was confirmed in several tissues. For histological analysis, $Sppl2a^{-/-}$ mice and wild-type littermates aged 7 to 14 days and 2 to 10 months old were euthanized in compliance with National and International Standards and approved by the Institutional Review Board for Animal Care.

Histological procedures

Mice were anesthetized by intraperitoneal (i.p.) injection of xylazine/ketamine and perfused transcardially with 6% (wt/vol) glutaraldehyde in 0.1 M phosphate buffer, pH 7.4. Jaws were removed, demineralized with EDTA, postfixed with 2% OsO_4, and embedded in Epon according to routine methods. Semi-thin sections (1 μm) were stained with toluidine blue. For transmission electron microscopy, ultrathin sections were counterstained with uranyl acetate and lead citrate. Alternatively, jaws from euthanized mice were fixed by immersion in 5% paraformaldehyde in 0.1 M phosphate buffer pH 7.3 overnight, decalcified in 4.2% EDTA, pH 7.3 for 2 to 3 weeks at 4°C, and embedded in paraffin or methylmethacrylate (MMA) resin. Sagittal serial sections 5 to 7-μm-thick were cut, mounted on polylysine-coated glass slides and stained with hematoxylin or hematoxylin-eosin.

Apoptotic cell counting

Sagittal MMA and paraffin sections containing late secretion stage through early maturation stage were used. Using transitional ameloblasts as landmarks, ameloblasts with condensed or fragmented nuclei that stained intensely dark blue with hematoxylin were counted at ×200 magnification within a stretch extending 300 μm in the apical direction and 300 μm in the incisal direction. Clusters of at least three nuclear fragments within a radius of 10 μm were assumed to originate from one apoptotic nucleus and were also included. In a previous study, ameloblasts exhibiting these specific changes had been shown to be positive for DNA fragments when stained with the terminal deoxynucleotidyl transferase–mediated deoxyuridine triphosphate-biotin nick end labeling (TUNEL) method and, thus, to represent apoptotic cells.[10]

Immunohistochemical detection of SPPL2A

A polyclonal antiserum for detection of SPPL2A was raised in rabbits against a synthetic peptide from the N-terminal (luminal) domain of SPPL2A (mouse sequence residues 77–94), affinity-purified using the immobilized peptide, and validated appropriately as described.[6,8] Paraffin sections were dewaxed in xylene and rehydrated in a descending series of ethanol. Immunohistochemical detection of SPPL2A required antigen retrieval by 1 mM ethylene glycol tetraacetic acid (EGTA) at pH 9.0, at 60°C overnight, and was performed with the Envision kit (Dakocytomation, Glostrup, Denmark) based on horseradish peroxidase and diaminobenzidine. Specificity of the procedure was controlled by staining sections derived from *Sppl2a* null mice as well as by replacing the primary antibody with normal rabbit control immunoglobulin G (IgG).

Micro–computed tomography

Blocks of MMA-embedded mouse hemimandibles were trimmed and scanned at a resolution of 8 μm voxels using a micro–computed tomography (μCT)-40 high-resolution scanner (Scanco Medical, AG, Bassersdorf, Switzerland) to analyze the

degree of mineral content in the enamel. From the collected images, a three-dimensional (3D) computer reconstruction of the jaws was made. Then a series of virtual cross-sections of 400-µm-thick slices was constructed throughout the length of the incisor. In each slice, the density of enamel, (crown) dentin, and surrounding alveolar bone was measured (spot area about 10 to 50 µm in diameter, depending on the available surface area). The mineral density was quantified at three locations throughout the enamel thickness: at the lateral, central, and mesial side of the enamel (Fig. 2). For each animal and for each slice, an overall enamel density value was calculated as the mean of these three single values. The slice values from 3 mice per genotype were averaged (mean and SD) and plotted as a function of development stage (increasing slice number). The values of each of the selected sites were also plotted to examine the changes in either lateral, central, or mesial sides of the enamel. Calibration was done with a series of hydroxyapatite phantoms with the following densities: 0, 0.1, 0.2, 0.4., 0.8, and 1.2 g hydroxyapatite/cm^3 (the last density was the highest density commercially possible). It should be noted that these graphs represent only relative values.

Elemental analysis by electron probe microanalysis

For quantified elemental analysis of enamel, undecalcified jaws were embedded in epoxy resin, polished, and coated with graphite. Measurements were performed on a JEOL Superprobe JXA-8900R electron microprobe (Institute of Geosciences, University of Kiel, Kiel, Germany), equipped with five wavelength dispersive spectrometers. The accelerating voltage was 15 kV or 20 kV for a beam current of 20 nA. Synthetic and natural mineral standards were used. Sample spot sizes were 1 to 5 µm in diameter. The raw data were corrected using the CITZAF method of Armstrong.[11] Enamel in advanced maturation stage apical from the alveolar bone crest was analyzed along with underlying dentine for CaO, P_2O_5, MgO, Na_2O, K_2O, FeO, and Cl ($n = 4$ animals per genotype, one upper and lower incisor) by performing line scans through the whole enamel thickness (spot distance 8 µm) and the underlying dentin (spot distance 50 µm). Mean values for weight percent were statistically tested using an unpaired two-tailed t test ($^*p < 0.05$ and $^{**}p < 0.01$).

Results

Incisors of *Sppl2a* knockout mice are decolorized

Upon phenotypic analysis of *Sppl2a*$^{-/-}$ mice, we noticed that their incisors were chalky white opaque (lower incisor) or only slightly orange colored (upper incisors) in contrast to the deep orange stain seen in incisors of wild-type mice (Fig. 1*A*). Furthermore, most of the enamel layer appeared to be rapidly eroded after eruption (Fig. 1*A*, arrows) exposing the dentin at the incisal end of the teeth, which appeared worn off and blunt. Molars were not as clearly affected, but cusps seemed to be more eroded than in age-matched wild-type controls (Supporting Information Fig. S1A, B). These macroscopic observations indicated significant defects of tooth enamel formation in the absence of SPPL2A, leading to significantly reduced mechanical strength.

Expression of SPPL2A in the enamel organ

We started to explore the role of the protease SPPL2A in tooth formation by analyzing its expression in developing incisors

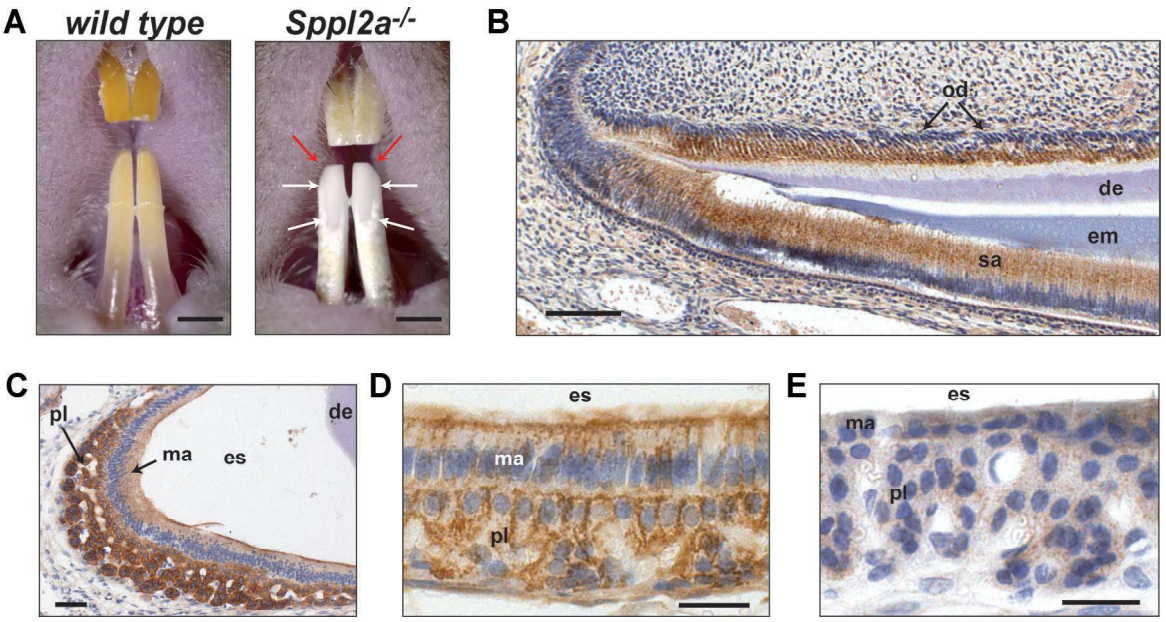

Fig. 1. SPPL2A is essential for tooth enamel formation. (*A*) Dental phenotype of *Sppl2a*$^{-/-}$ mice. Enamel from upper incisors of *Sppl2a* null mice is of weakly orange color whereas that of lower incisors is chalky white. The tips are blunt and most of the enamel has been eroded after eruption exposing the dentin (red arrow). White arrows point to the rim of the remaining enamel layer. In wild-type controls, the tips of the incisors are pointed, and the enamel is of orange/brown color. Scale bar = 1 mm. (*B–D*) Expression of SPPL2A was visualized immunohistochemically in incisors of wild-type mice. (*B*) SPPL2A was detected in secretory ameloblasts (sa) and odontoblasts (od). Scale bar = 100 µm. (*C*, *D*) In maturation stage, the cells of the papillary layer (pl) as well as ameloblasts (ma) were positive for SPPL2A. Scale bars = 50 µm (*C*) and 25 µm (*D*, *E*), respectively. (*E*) No staining for SPPL2A was observed in enamel organ cells of *Sppl2a*$^{-/-}$ mice, confirming specificity of the primary antibody employed. de = dentin; em = enamel matrix; es = enamel space.

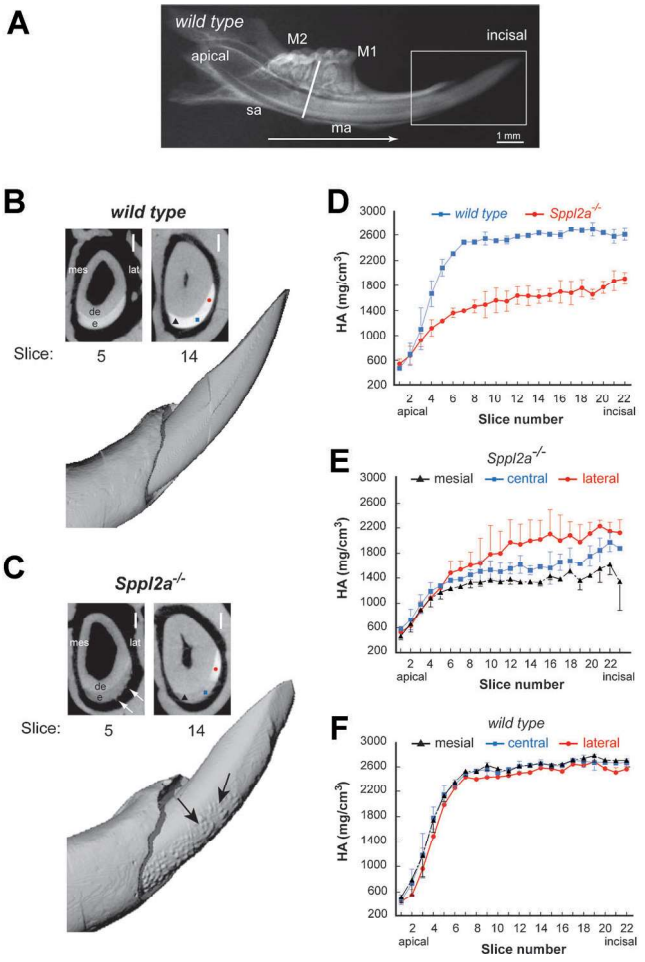

Fig. 2. Microcomputer tomography revealed delayed and inhomogeneous mineralization in lower incisors of *Sppl2a* knockout mice. (*A*) Low-power X-ray image of a lower incisor of a wild-type mouse. At the apical end, dental cells are generated that in incisal (arrow) direction differentiate into secretory ameloblasts (sa) and subsequently into maturation ameloblasts (ma). The line between the first (M1) and second (M2) molar is the approximate location where secretory ameloblasts have just transformed into maturation ameloblasts. The rectangular area presents the tip presented as 3D reconstructions. (*B*, *C*) Representative cross-sections from early maturation (slice #5) or late maturation stage (slice #14) and 3D reconstructions of a lower incisor from a wild-type (*B*) or *Sppl2a* null (*C*) mouse (Scale bars = 200 µm). The enamel surface in the *Sppl2a*$^{-/-}$ incisor was uneven and bumpy (arrows). Comparison of the respective cross-sections from both genotypes shows the substantial delay in enamel mineralization across the entire width of enamel in the *Sppl2a*$^{-/-}$ incisor and the difference in mineral content between lateral (lat, right) and mesial (mes, left) sides. (*D*–*F*) Relative quantification of mineral density in slices from apical (left) to incisal (right). Slices 1 to 3 and 4 to 18 represent the secretory and maturation stage, respectively. (*D*) The average density value of enamel in wild-type (blue) and *Sppl2a*$^{-/-}$ (red) lower incisors is plotted against successive stages of development and shows the relative delay in mineralization in enamel of *Sppl2a* null mice. (*E*, *F*) Comparison of the density values for either mesial (black triangles), central (blue squares), and lateral (red circles) enamel in *Sppl2a*$^{-/-}$ (*E*) or wild-type control incisors (*F*), respectively. Mean ± SD, $n = 3$ mice/group. de = dentin; e = enamel.

(Fig. 1*B*–*E*) and molars (not shown) of wild-type mice by immunohistochemistry. Expression of SPPL2A was detected in odontoblasts as well as ameloblasts (Fig. 1*B*). In the latter, SPPL2A was present during secretory and maturation stage (Fig. 1*B*, *C*). The cytoplasm of secretory ameloblasts exhibited fine granular staining for SPPL2A evenly distributed in the supranuclear area of the cells, which is compatible with the reported localization of SPPL2A in membranes of lysosomes and late endosomes detected in murine embryonic fibroblasts.[6] In maturation stage ameloblasts, SPPL2A immunostaining was mainly confined to the apical pole of the cells facing the forming enamel (Fig. 1*D*). Whether this indicates localization of SPPL2A in the apical plasma membrane or in plasma membrane–adjacent intracellular vesicles such as endosomal compartments, cannot be clearly distinguished at this level of resolution. During maturation phase very strong SPPL2A expression was observed in the epithelial cells of the papillary layer (Fig. 1*C*, *D*). Specificity of the employed SPPL2A antibody was confirmed by replacement of the primary antibody by normal rabbit IgG (not shown) or by staining of sections from incisors of *Sppl2a*$^{-/-}$ mice (Fig. 1*E*). In both cases no signals were detected.

Hypomineralization of enamel in *Sppl2a*$^{-/-}$ mice

Having confirmed that SPPL2A is expressed in cell types generating enamel and dentin, we sought to more precisely define the defects in incisors of *Sppl2a* null mice by µCT analysis of mandibles (Fig. 2). In 3D reconstructions, macroscopic findings regarding blunting and enamel erosion were recapitulated (Fig. 2*A*–*C*). The surface of the erupted enamel, which was smooth and regular in wild-type incisors, was uneven and bumpy in incisors from *Sppl2a* null mice.

We compared the mineral density of the different mineralized tissues present in the analyzed specimen. With respect to bone and dentin, the mineralization was very similar in wild-type and *Sppl2a* knockout mice. In contrast, the enamel of the mandibular incisors of *Sppl2a*$^{-/-}$ mice was less mineralized than that of wild-type mice (Fig. 2*D*). The difference in mineral content was already present at early maturation (Fig. 2*D*) and became more significant at advanced stages. In molars, the mineral density of enamel was also found to be significantly reduced in *Sppl2a*$^{-/-}$ versus wild-type mice (Supporting Information Fig. S1C). However, the hypomineralization appeared to be slightly less pronounced in molars than in incisors. Remarkably, the degree of hypomineralization in cross-sections of *Sppl2a*$^{-/-}$ incisors was not homogenous. Enamel at the mesial side exhibited a significantly lower mineral density than enamel at the lateral side (Fig. 2*E*), with intermediate values observed for the central enamel. These differences became even more prominent as amelogenesis progressed (Fig. 2*E*). In contrast, no inhomogeneity of mineral density was detected in wild-type incisors (Fig. 2*F*).

We also analyzed the ultrastructure of enamel from *Sppl2a*$^{-/-}$ mice by backscatter electron microscopy (Fig. 3*A*) and found that, in general, the rod structure was regular and comparable to that of wild-type mice. However, at several sites of *Sppl2a*$^{-/-}$ incisors a fracture line was observed within the outer enamel leading to a splitting of the outer enamel (Fig. 3*A*, arrow) and most probably

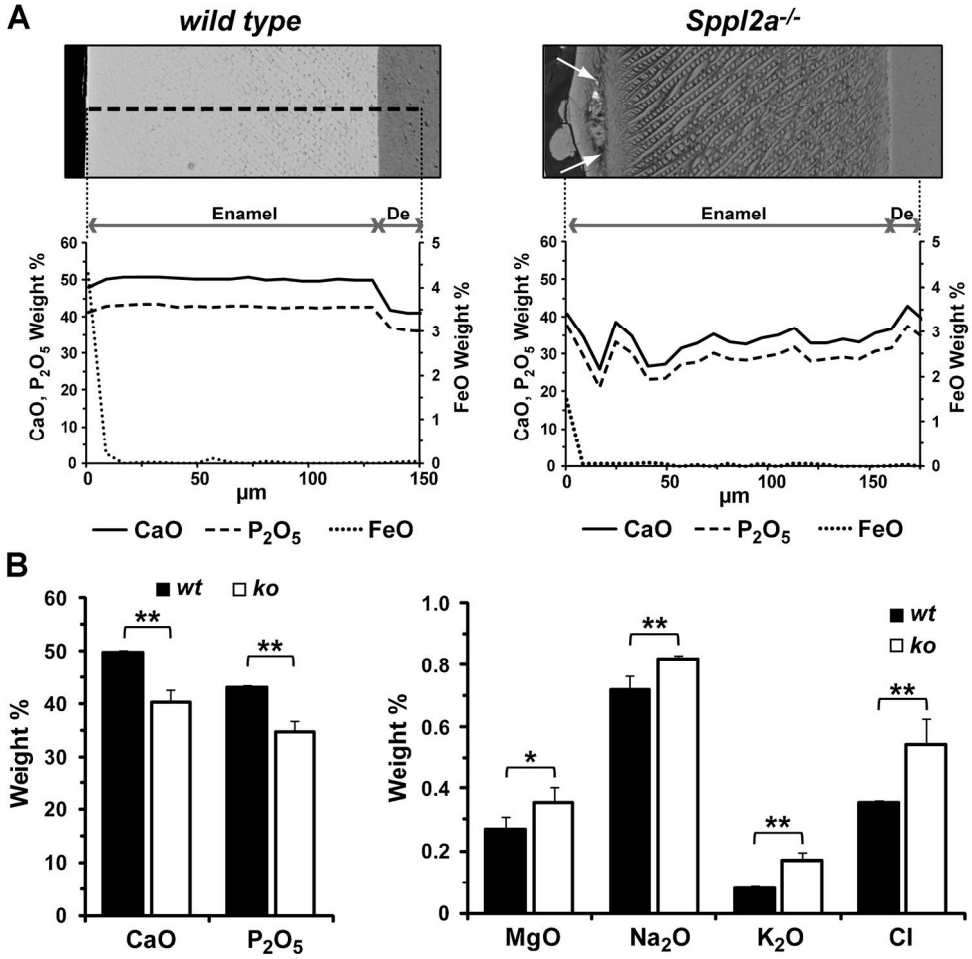

Fig. 3. Structural analysis and quantification of elemental composition of enamel from *Sppl2a*$^{-/-}$ incisors. (*A*) Backscatter electron microscopy of enamel from wild-type and *Sppl2a*$^{-/-}$ incisors reveals a characteristic disruption of the outer enamel and splitting into two layers in *Sppl2a* knockout mice (arrows). Line scans from the enamel surface to the dentin enamel junction were performed as indicated on wild-type and *Sppl2a*$^{-/-}$ enamel and weight % of CaO, P_2O_5, and FeO were determined for spots every 8 µm (enamel) or every 50 µm (dentin, De). In agreement with the macroscopically observed decolorization of *Sppl2a*$^{-/-}$ enamel, the iron content at the enamel surface was reduced as compared to the control. In wild-type mice iron depositions are known to account for the characteristic yellow/orange color of the incisors. (*B*) Quantification of mineral content (weight % of CaO, P_2O_5, MgO, Na_2O, K_2O, and Cl) of enamel from wild-type and *Sppl2a* null mice ($n = 4$ mice per genotype) by electron microprobe analysis depicted as mean ± SD ($^{**}p < 0.01$, $^{*}p < 0.05$, unpaired, two-tailed *t* test). Enamel from *Sppl2a*$^{-/-}$ incisors contained significantly less calcium and phosphorus than wild-type enamel being in line with the relative quantification of mineral density by microcomputer tomography. In contrast, abundance of minor enamel constituents such as magnesium, sodium, potassium, and chloride was significantly increased in the enamel from *Sppl2a* knockout mice.

accounting for the irregular enamel surface visualized in the 3D reconstruction of the µCT data (Fig. 2*C*).

Elemental composition of enamel was determined using quantitative electron probe microanalysis by performing line scans perpendicular from the enamel surface to the dentin-enamel junction, as shown, from a representative measurement in Fig. 3*A* or as mean ± SD in Fig. 3*B*. The measured calcium and phosphorus content was very constant over the whole thickness of the enamel in wild-type incisors. However, *Sppl2a*$^{-/-}$ incisors exhibited significant variation and irregularity in the line scans carried out across the enamel. Altogether, the calcium and phosphorus content in the enamel of these teeth was reduced to ~80% of the wild-type level, confirming the findings from µCT (Fig. 2). In return, abundance of magnesium, sodium, potassium, and chloride was slightly, though significantly, increased in *Sppl2a*$^{-/-}$ enamel (Fig. 3*B*). As an equivalent of the macroscopically observed decolorization of *Sppl2a*$^{-/-}$ incisors, we found that iron—well detectable in the most superficial enamel layer of wild-type incisors—was less abundant at the surface of *Sppl2a*$^{-/-}$ enamel (Fig. 3*A*). In dentin, no reduction of calcium and phosphorus levels was detected in incisors from *Sppl2a* null mice (not shown).

Characteristic histological changes of maturation stage ameloblasts in *Sppl2a*$^{-/-}$ mice

To provide insight into why enamel produced in the absence of SPPL2A is not adequately mineralized, we examined the morphology of the enamel organs during different stages of amelogenesis in mandibular incisors of *Sppl2a* null mice (Fig. 4). Because enamel thickness (Fig. 4*A*) and rod structure (Fig. 4*B*) were not affected by the absence of

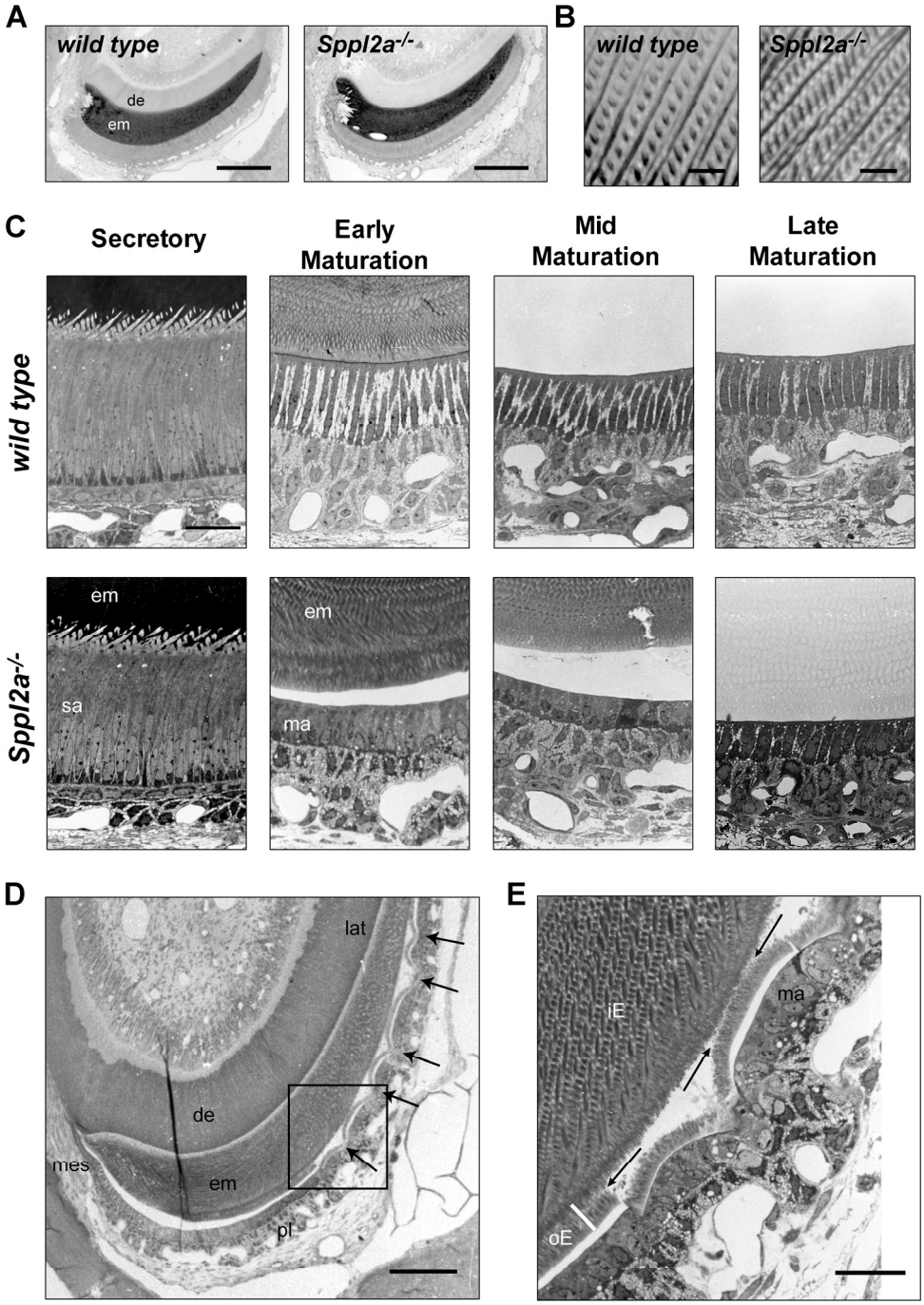

Fig. 4. Histological changes in dental epithelium of *Sppl2a* knockout mice. (*A*–*C*) Representative semi-thin sections of lower incisors from wild-type and *Sppl2a* null (*Sppl2a*$^{-/-}$) mice embedded in Epon and stained with toluidine blue. Cross-sections of the late secretory zone showed that the amount (*A*) and structure (*B*) of the enamel matrix secreted by *Sppl2a*$^{-/-}$ ameloblasts was equivalent to that in wild-type incisors. Scale bars = 200 µm (*A*) or 10 µm (*B*), respectively. (*C*) Ameloblast morphology was assessed in zones of secretory as well as early, mid, or late maturation stage amelogenesis. The histological appearance of secretory ameloblasts was similar in mice from both genotypes. During maturation stage, a delayed and incomplete disappearance of stainable material in the enamel space was observed in *Sppl2a*$^{-/-}$ incisors indicating persistence of residual enamel matrix. Furthermore, the ameloblast layer in *Sppl2a*$^{-/-}$ incisors was reduced in height. The detachment of ameloblasts from the enamel surface was considered to be an artifact due to the dissection of the specimens and was observed in samples from both genotypes at comparable frequency. Scale bar = 25 µm. (*D*, *E*) Undulation and localized degeneration of maturation stage ameloblasts in *Sppl2a*$^{-/-}$ mice. (*D*) Enamel organ in the region of early maturation stage. The outer enamel layer shows splitting and several firm focal adhesions (arrows) to ameloblasts in the lateral (lat) region of the enamel organ. (*E*) One adhesion point marked in *D* is presented at higher resolution. At the site of firm adhesion, the maturation stage ameloblasts (ma) appeared disorganized. Long arrows point to the fissure within the outer enamel (oE). The apparent dissociation of the outer enamel from the ameloblasts outside the firm adhesions is most probably an artifact. The pattern of the inner enamel (iE) resembles that of controls. Scale bars = 50 µm (*D*) and 25 µm (*E*), respectively. de = dentin; em = enamel matrix; sa = secretory ameloblast; ma = maturation stage ameloblast; mes = mesial; pl = papillary layer.

SPPL2A, there was no indication of any functional deficit during the secretory stage of amelogenesis in these mice. Consequently, we observed no morphological differences between secretory stage ameloblasts in wild-type and *Sppl2a*$^{-/-}$ mice (Fig. 4*C*).

During enamel maturation, one of the main processes is the gradual removal of the organic matrix. This is a prerequisite for the gradual augmentation of the enamel rods and thus for complete mineralization.[12] Histologically, the matrix removal leads to optically empty enamel spaces, when EDTA-treated tissue blocks are used. In semi-thin sections (1 μm) of wild-type incisors, the matrix completely disappeared during the stage of early maturation. In contrast, significant amounts of matrix were still present at late maturation stage in *Sppl2a*$^{-/-}$ incisors (Fig. 4*C*). This indicates that resorption of the enamel matrix is impaired in incisors of *Sppl2a* knockout mice.

Initial morphological changes of *Sppl2a* null ameloblasts were observed in the transition zone from secretory to maturation stage. There, an increased number of ameloblasts with apoptotic nuclei and nuclear fragments in *Sppl2a*$^{-/-}$ mice was conspicuous (5.6 ± 0.6 cells in *Sppl2a*$^{-/-}$ versus 1.8 ± 1.2 cells in wild-types, $p < 0.05$). Throughout all maturation stages, *Sppl2a*$^{-/-}$ ameloblasts exhibited reduced height compared to controls (Fig. 4*C*). Intercellular spaces between ameloblasts, which were prominent in wild-type incisors, were in many instances hardly visible in *Sppl2a*$^{-/-}$ incisors at the level of light microscopy.

We have also performed transmission electron microscopy in order to compare wild-type and *Sppl2a*$^{-/-}$ maturation stage ameloblasts at the level of ultrastructure. Specifically, we examined the abundance and structure of subcellular organelles, the pattern of the enamel matrix, the presence of basal-lamina-like structures and associated hemidesmosomes, and intercellular contacts like desmosomes or gap junctions either between ameloblasts or papillary cells or between both cell types (not shown). However, no consistent differences between wild-type and *Sppl2a*$^{-/-}$ mice were seen. In contrast, concerning the modulation of maturation stage ameloblasts between the ruffled-ended and smooth-ended state,[12] differences were observed (not shown). In wild-type incisors, both states were encountered, with the ruffled-ended state occurring much more frequently than the smooth-ended state. In *Sppl2a* null ameloblasts, a few invaginations of the apical plasma membrane were observed in some ameloblasts reminiscent of the ruffled-ended state; typical smooth-ended ameloblasts were not found (not shown).

A very conspicuous feature of *Sppl2a* null incisors was the splitting of the outer enamel into two halves. This was detected predominantly on the lateral side of the enamel organ (Fig. 4*D*). At these sites, the ameloblast layer exhibited an undulated pattern due to funnel-like invaginations into the papillary layer, the epithelium was disorganized and the ameloblasts appeared degenerated. Furthermore, at these invaginations the apical plasma membrane of the ameloblasts seemed to be strongly adherent to the outermost layer of the outer enamel that had been detached from the bulk of enamel (Fig. 4*E*). At these sites, the splitting of the outer enamel was particularly prominent, suggesting that the invaginating ameloblasts applied traction on the outer enamel contributing to the observed disruption of this layer.

Discussion

The dental changes in *Sppl2a* knockout mice reveal that the intramembrane protease SPPL2A is essential to maintain cellular homeostasis of ameloblasts. In the absence of this protein, maturation stage ameloblasts undergo significant structural changes. This is associated with a loss of function as demonstrated by the impaired resorption of enamel matrix, which is considered as an absolute prerequisite for the completion of enamel mineralization.[12,13] The observed phenotype of *Sppl2a*$^{-/-}$ mice does not necessarily indicate a direct function of SPPL2A in matrix resorption, but rather a general importance of this protease for maintaining ameloblasts. Proteins involved in diverse cellular processes and pathways have been implicated in ameloblast homeostasis, based on ameloblast dysfunction/degeneration in mice deficient for the respective protein. Examples for this are the transcription factors/regulators Nuclear factor erythroid 2-related factor 2 (Nrf 2)[14] and muscle segment homeobox gene 2 (Msx2)[15] or the lipid biosynthetic enzyme 1-acyl-sn-glycerol-3-phosphate acyltransferase beta (AGPAT2).[16] In agreement with these models, the phenotype of *Sppl2a*$^{-/-}$ mice further corroborates the absolute requirement of maturation stage ameloblasts and their cellular activity for matrix resorption and enamel mineralization. According to our knowledge, SPPL2A is the first example of an intramembrane protease being implicated in tooth formation.

There is significant similarity between the enamel of *SPPL2a*$^{-/-}$ mice and that of kallikrein 4 null (*Klk4*$^{-/-}$) mice.[17–20] Absence of SPPL2A or KLK4 does not change the thickness of enamel layer or the enamel prism structure but is associated with impaired resorption of the enamel matrix and consecutively hypomineralized enamel. It is well conceivable that secretion of KLK4 at maturation stage is reduced in *Sppl2a*$^{-/-}$ mice due to the described ameloblast dysfunction and that this contributes to the delayed maturation of dental enamel.

A very unique feature of the phenotype in *Sppl2a* null incisors is the splitting of the outer enamel. This may suggest defects in the enamel matrix, which is secreted during the late secretory stage of enamel formation just prior to the start of maturation. Interestingly, we have detected expression of SPPL2A throughout secretory as well as maturation stage ameloblasts. Apparently, there is a latency period until the loss of SPPL2A negatively affects ameloblast's function and morphology. Because ameloblasts substantially remodel their morphology, function, and gene expression profiles from secretory until late maturation stage,[21,22] SPPL2A may be responsible for cleaving different substrates during the respective stages. Expression of SPPL2A was very high in cells of the papillary layer, which have been suggested to form a functional syncytium with the modulating ameloblasts.[23] Therefore, it cannot be excluded that the loss of SPPL2A functions in the papillary layer cells contributes to the ameloblast dysfunction.

Endocytic activity is assumed to play a major role for the removal of enamel matrix—either by direct uptake of matrix proteins or by clearance of breakdown products resulting from the action of extracellular proteases.[12] Recently, it was demonstrated that a number of endocytosis-related as well as lysosomal proteins were upregulated in maturation stage

ameloblasts.[24] Conspicuously, SPPL2A is localized in membranes of lysosomes and late endosomes. The actual substrate of SPPL2A in enamel organ cells is currently unknown. Mechanistically, the absence of SPPL2A may negatively influence ameloblast homeostasis by the loss of certain signals that are transduced by intracellular domains released from substrates by the proteolytic activity of SPPL2A. Alternatively, non-cleaved substrates may accumulate in the absence of this protease and exert adverse effects as in the case of CD74.[8]

Altogether, four substrates of SPPL2A have been identified. Whereas the identification of tumor necrosis factor α (TNFα),[7,25] the Fas ligand (FasL),[26] and the Bri2 protein[27] is so far merely based on in vitro cell-culture approaches, CD74[8] has been validated in vivo in *Sppl2a*$^{-/-}$ mice. None of these proteins has a clearly documented role in amelogenesis. FasL binds to its receptor Fas, which induces apoptosis. In early stage of morphogenesis dental epithelium expresses both Fas and FasL,[28,29] but very little information is available on expression of these factors at later stages of amelogenesis. Ameloblasts in secretory and maturation stage did not immunostain for TNFα but were positive for Fas.[30] Papillary cells and stratum intermedium stained weakly for FasL, but FasL could not be detected by Western blotting.[30] Based on the finding that *Sppl2a* null ameloblasts seem to undergo more apoptosis than controls, the expression and role of FasL and TNFα in ameloblasts should be reexamined and both proteins evaluated as potential candidate substrates of SPPL2A in ameloblasts.

Under noninflammatory conditions, CD74 is primarily expressed in MHCII-positive antigen-presenting cells.[31] We showed recently that the B cell phenotype of *Sppl2a*$^{-/-}$ mice was significantly alleviated in *Sppl2a*$^{-/-}$ *Cd74*$^{-/-}$ mice, proving the causative role of accumulating CD74 N-terminal fragments.[8] However, decolorization and enamel erosion of incisors in Sppl2a-Cd74 double-knockout mice was macroscopically indistinguishable from that seen in *Sppl2a*$^{-/-}$ mice, showing no amelioration of enamel maturation by additional *Cd74* ablation (not shown). Furthermore, we also examined incisors of *Cd74*$^{-/-}$ mice in comparison to those of wild-type mice and observed no macroscopically detectable changes in enamel color or enamel stability (not shown). Therefore, no indication was obtained for any functional link between CD74 as SPPL2A substrate and the impairment of enamel maturation in the absence of SPPL2A.

It is conceivable that this phenotype is related to a novel, yet unrecognized substrate of SPPL2A. More than 1400 type II transmembrane proteins[32] were identified by bioinformatic approaches in the mouse genome constituting the pool of theoretical SPPL2A substrates due to their membrane topology. Based on their documented role in either tooth morphogenesis or the formation of enamel or other mineralized tissues, respectively, we have specifically analyzed the type II transmembrane proteins ectodysplasin (EDA),[33] collagen 17A (COL17A),[34] and RANKL (TRANCE)[35] as putative substrates of SPPL2A by coexpressing them with the protease in HeLa cells. However, no conclusive evidence was obtained that any of these proteins, either as full-length form or as N-terminal fragment, are cleaved by SPPL2A (not shown). Thus, further studies will be needed to elucidate the precise molecular function of SPPL2A in ameloblasts.

In conclusion, we have identified the intramembrane protease SPPL2A as a novel key player in tooth enamel generation by being essential for preserving cellular homeostasis of ameloblasts during maturation stage of enamel formation. In light of SPPL2A as a promising drug target for depleting and/or functionally modulating B cells by pharmacological inhibition of this protease in order to treat autoimmune disorders, impairment of ameloblast function and thus formation of tooth enamel will have to be considered as a putative adverse effect. This may preclude the use of respective inhibitors in children up to the age enamel formation of the permanent dentition has been completed.

Disclosures

All authors state that they have no conflicts of interest.

Acknowledgments

This work was supported by the Deutsche Forschungsgemeinschaft as part of the SFB 877. We acknowledge the technical support from Marion van Duin and Mark Schoonderwoerd (Oral Cell Biology ACTA, Amsterdam), Peter Brugman (Functional Anatomy, ACTA, Amsterdam), Dagmar Niemeier (Institute of Anatomy, Christian-Albrechts-University, Kiel), and Marlies Rusch (Biochemical Institute, Christian-Albrechts-University, Kiel). We thank Dietmar Detlef for help with sample preparation, Dr. Peter Appel and Barbara Mader for help with electron microprobe analysis (Institute of Geology, Christian-Albrechts-University, Kiel), Dr. Jing Guo (ACTA, Amsterdam) for support with μCT measurements, and Dr. Charles Smith (McGill, Montreal Canada) for many helpful remarks in preparing this manuscript.

Authors' roles: AB, RL, and BS designed the experiments. AB, NG, RL, JS, AM, NH, and TB performed the experiments. AB, RL, and BS analyzed the data. RF, VE, and PS gave significant conceptual advice. AB, RL, and BS wrote the manuscript. All authors read, edited, and approved the final manuscript. BS takes responsibility for the integrity of the data analysis.

References

1. Lichtenthaler SF, Haass C, Steiner H. Regulated intramembrane proteolysis—lessons from amyloid precursor protein processing. J Neurochem. 2011;117:779–96.
2. Urban S, Freeman M. Intramembrane proteolysis controls diverse signalling pathways throughout evolution. Curr Opin Genet Dev. 2002;12:512–8.
3. De Strooper B, Annaert W, Cupers P, Saftig P, Craessaerts K, Mumm JS, Schroeter EH, Schrijvers V, Wolfe MS, Ray WJ, Goate A, Kopan R. A presenilin-1-dependent gamma-secretase-like protease mediates release of Notch intracellular domain. Nature. 1999;398:518–22.
4. Wolfe MS, Kopan R. Intramembrane proteolysis: theme and variations. Science. 2004;305:1119–23.
5. Fluhrer R, Steiner H, Haass C. Intramembrane proteolysis by signal peptide peptidases: a comparative discussion of GXGD-type aspartyl proteases. J Biol Chem. 2009;284:13975–9.
6. Behnke J, Schneppenheim J, Koch-Nolte F, Haag F, Saftig P, Schröder B. Signal-peptide-peptidase-like 2a (SPPL2a) is targeted to lysosomes/late endosomes by a tyrosine motif in its C-terminal tail. FEBS Lett. 2011;585:2951–7.

7. Friedmann E, Hauben E, Maylandt K, Schleeger S, Vreugde S, Lichtenthaler SF, Kuhn PH, Stauffer D, Rovelli G, Martoglio B. SPPL2a and SPPL2b promote intramembrane proteolysis of TNFalpha in activated dendritic cells to trigger IL-12 production. Nat Cell Biol. 2006;8:843–8.
8. Schneppenheim J, Dressel R, Hüttl S, Lüllmann-Rauch R, Engelke M, Dittmann K, Wienands J, Eskelinen EL, Hermans-Borgmeyer I, Fluhrer R, Saftig P, Schröder B. The intramembrane protease SPPL2a promotes B cell development and controls endosomal traffic by cleavage of the invariant chain. J Exp Med. 2013;210:41–58.
9. Hu JC, Chun YH, Al Hazzazzi T, Simmer JP. Enamel formation and amelogenesis imperfecta. Cells Tissues Organs. 2007;186:78–85.
10. Bronckers AL, Lyaruu DM, Goei W, Litz M, Luo G, Karsenty G, Woltgens JH, D'Souza RN. Nuclear DNA fragmentation during postnatal tooth development of mouse and hamster and during dentin repair in the rat. Eur J Oral Sci. 1996;104:102–11.
11. Armstrong JT. Citzaf: a package of correction programs for the quantitative electron microbeam x-ray-analysis of thick polished materials, thin-films, and particles. Microbeam Anal. 1995;4:177–200.
12. Smith CE. Cellular and chemical events during enamel maturation. Crit Rev Oral Biol Med. 1998;9:128–61.
13. Simmer JP, Richardson AS, Hu YY, Smith CE, Ching-Chun HJ. A post-classical theory of enamel biomineralization … and why we need one. Int J Oral Sci. 2012;4:129–34.
14. Yanagawa T, Itoh K, Uwayama J, Shibata Y, Yamaguchi A, Sano T, Ishii T, Yoshida H, Yamamoto M. Nrf2 deficiency causes tooth decolourization due to iron transport disorder in enamel organ. Genes Cells. 2004;9:641–51.
15. Satokata I, Ma L, Ohshima H, Bei M, Woo I, Nishizawa K, Maeda T, Takano Y, Uchiyama M, Heaney S, Peters H, Tang Z, Maxson R, Maas R. Msx2 deficiency in mice causes pleiotropic defects in bone growth and ectodermal organ formation. Nat Genet. 2000;24:391–5.
16. Vogel P, Read R, Hansen G, Wingert J, Dacosta CM, Buhring LM, Shadoan M. Pathology of congenital generalized lipodystrophy in Agpat2$^{-/-}$ mice. Vet Pathol. 2011;48:642–54.
17. Smith CE, Richardson AS, Hu Y, Bartlett JD, Hu JC, Simmer JP. Effect of kallikrein 4 loss on enamel mineralization: comparison with mice lacking matrix metalloproteinase 20. J Biol Chem. 2011;286:18149–60.
18. Simmer JP, Hu Y, Richardson AS, Bartlett JD, Hu JC. Why does enamel in Klk4-null mice break above the dentino-enamel junction?. Cells Tissues Organs. 2011;194:211–5.
19. Yamakoshi Y, Richardson AS, Nunez SM, Yamakoshi F, Milkovich RN, Hu JC, Bartlett JD, Simmer JP. Enamel proteins and proteases in Mmp20 and Klk4 null and double-null mice. Eur J Oral Sci. 2011;119 (Suppl 1):206–16.
20. Hu Y, Hu JC, Smith CE, Bartlett JD, Simmer JP. Kallikrein-related peptidase 4, matrix metalloproteinase 20, and the maturation of murine and porcine enamel. Eur J Oral Sci. 2011;119(Suppl 1):217–25.
21. Lacruz RS, Smith CE, Bringas P Jr, Chen YB, Smith SM, Snead ML, Kurtz I, Hacia JG, Hubbard MJ, Paine ML. Identification of novel candidate genes involved in mineralization of dental enamel by genome-wide transcript profiling. J Cell Physiol. 2012;227:2264–75.
22. Lacruz RS, Smith CE, Chen YB, Hubbard MJ, Hacia JG, Paine ML. Gene-expression analysis of early- and late-maturation-stage rat enamel organ. Eur J Oral Sci. 2011;119(Suppl 1):149–57.
23. Josephsen K, Takano Y, Frische S, Praetorius J, Nielsen S, Aoba T, Fejerskov O. Ion transporters in secretory and cyclically modulating ameloblasts: a new hypothesis for cellular control of preeruptive enamel maturation. Am J Physiol Cell Physiol. 2010;299:C1299–307.
24. Lacruz RS, Brookes SJ, Wen X, Jimenez JM, Vikman S, Hu P, White SN, Lyngstadaas SP, Okamoto CT, Smith CE, Paine ML. Adaptor protein complex 2 (AP-2) mediated, clathrin dependent endocytosis, and related gene activities, are a prominent feature during maturation stage amelogenesis. J Bone Miner Res. 2013 Mar;28 (3):672–87.
25. Fluhrer R, Grammer G, Israel L, Condron MM, Haffner C, Friedmann E, Bohland C, Imhof A, Martoglio B, Teplow DB, Haass C. A gamma-secretase-like intramembrane cleavage of TNFalpha by the GxGD aspartyl protease SPPL2b. Nat Cell Biol. 2006;8:894–6.
26. Kirkin V, Cahuzac N, Guardiola-Serrano F, Huault S, Luckerath K, Friedmann E, Novac N, Wels WS, Martoglio B, Hueber AO, Zornig M. The Fas ligand intracellular domain is released by ADAM10 and SPPL2a cleavage in T-cells. Cell Death Differ. 2007;14:1678–87.
27. Martin L, Fluhrer R, Reiss K, Kremmer E, Saftig P, Haass C. Regulated intramembrane proteolysis of Bri2 (Itm2b) by ADAM10 and SPPL2a/SPPL2b. J Biol Chem. 2008;283:1644–52.
28. Kumamoto H, Kimi K, Ooya K. Immunohistochemical analysis of apoptosis-related factors (Fas, Fas ligand, caspase-3 and single-stranded DNA) in ameloblastomas. J Oral Pathol Med. 2001;30:596–602.
29. Matalova E, Svandova E, Tucker AS. Apoptotic signaling in mouse odontogenesis. OMICS. 2012;16:60–70.
30. Nishikawa S. Colchicine-induced apoptosis and anti-Fas localization in rat-incisor ameloblasts. Anat Sci Int. 2002;77:175–81.
31. Neefjes J, Jongsma ML, Paul P, Bakke O. Towards a systems understanding of MHC class I and MHC class II antigen presentation. Nat Rev Immunol. 2011;11:823–36.
32. Aturaliya RN, Fink JL, Davis MJ, Teasdale MS, Hanson KA, Miranda KC, Forrest AR, Grimmond SM, Suzuki H, Kanamori M, Kai C, Kawai J, Carninci P, Hayashizaki Y, Teasdale RD. Subcellular localization of mammalian type II membrane proteins. Traffic. 2006;7:613–25.
33. Miard S, Peterkova R, Vonesch JL, Peterka M, Ruch JV, Lesot H. Alterations in the incisor development in the Tabby mouse. Int J Dev Biol. 1999;43:517–29.
34. Asaka T, Akiyama M, Domon T, Nishie W, Natsuga K, Fujita Y, Abe R, Kitagawa Y, Shimizu H. Type XVII collagen is a key player in tooth enamel formation. Am J Pathol. 2009;174:91–100.
35. Ohazama A, Sharpe PT. TNF signalling in tooth development. Curr Opin Genet Dev. 2004;14:513–9.